PNAS RESEARCH ARTICLE | NEUROSCIENCE

Expression of the vesicular GABA transporter within neuromedin S$^+$ neurons sustains behavioral circadian rhythms

Ivana L. Bussi[a,1], Alexandra F. Neitz[a,b], Raymond E. A. Sanchez[a,c,2], Leandro P. Casiraghi[a,3], Michael Moldavan[d,e], Divya Kunda[a], Charles N. Allen[d,e], Jennifer A. Evans[f], and Horacio O. de la Iglesia[a,b,c,1]

Edited by Joseph Takahashi, The University of Texas Southwestern Medical Center, Dallas, TX; received August 30, 2023; accepted October 16, 2023

The suprachiasmatic nucleus (SCN) of the hypothalamus is the site of a central circadian clock that orchestrates overt rhythms of physiology and behavior. Circadian timekeeping requires intercellular communication among SCN neurons, and multiple signaling pathways contribute to SCN network coupling. Gamma-aminobutyric acid (GABA) is produced by virtually all SCN neurons, and previous work demonstrates that this transmitter regulates coupling in the adult SCN but is not essential for the nucleus to sustain overt circadian rhythms. Here, we show that the deletion of the gene that codes for the GABA vesicular transporter *Vgat* from neuromedin-S (NMS)$^+$ neurons—a subset of neurons critical for SCN function—causes arrhythmia of locomotor activity and sleep. Further, NMS-*Vgat* deletion impairs intrinsic clock gene rhythms in SCN explants cultured ex vivo. Although vasoactive intestinal polypeptide (VIP) is critical for SCN function, *Vgat* deletion from VIP-expressing neurons did not lead to circadian arrhythmia in locomotor activity rhythms. Likewise, adult SCN-specific deletion of *Vgat* led to mild impairment of behavioral rhythms. Our results suggest that while the removal of GABA release from the adult SCN does not affect the pacemaker's ability to sustain overt circadian rhythms, its removal from a critical subset of neurons within the SCN throughout development removes the nucleus ability to sustain circadian rhythms. Our findings support a model in which SCN GABA release is critical for the developmental establishment of intercellular network properties that define the SCN as a central pacemaker.

suprachiasmatic | GABA | *Vgat* | sleep

Significance

In mammals, the suprachiasmatic nucleus (SCN) houses a central circadian clock that governs physiological and behavioral rhythms. Virtually, all neurons in the SCN release the neurotransmitter GABA (Gamma-aminobutyric acid). Surprisingly, blocking GABAergic transmission in the adult affects interneuronal coupling but does not impair the SCN's ability to sustain circadian rhythms. In contrast, here, we show that genetically impairing the release of GABA in a critical subset of SCN neurons throughout development leads to total circadian arrhythmia in most animals. This impairment of circadian rhythmicity is manifested as arrhythmic circadian behavior and sleep, as well as disrupted circadian gene expression in the SCN. We postulate that GABAergic transmission throughout development is critical for the assembly of a functional central circadian pacemaker.

In mammals, circadian rhythms of behavior and physiology are driven by the suprachiasmatic nucleus (SCN) of the hypothalamus. SCN neurons display endogenous, self-sustained oscillations in gene expression and neurophysiology that are generated by auto-regulatory transcriptional–translational negative feedback loops involving "clock genes" (1). Isolated SCN neurons oscillate with a range of different periods relative to one another, but as a coupled population they display synchronized periods to drive coherent tissue-level rhythms (2). In addition to period synchrony, intercellular coupling among SCN neurons regulates the precision, amplitude, and robustness of cellular rhythms (3, 4). Last, SCN coupling allows for coordination of population-level phasing of cellular rhythms in response to changes in the photic environment (5–7). To support these emergent network functions, SCN neurons interact through multiple signaling mechanisms.

Gamma-aminobutyric acid (GABA) is expressed by nearly all SCN neurons in both rodents and humans (8–10), yet the mechanisms through which this neurotransmitter influences SCN network properties have yet to be fully determined (11). GABA application phase shifts and synchronizes SCN neurons dissociated in culture (12), and GABA signaling can contribute to phase coordination at the network level as well as to photic responses and environmental encoding by the SCN circadian pacemaker (13–19). Interestingly, GABA can also destabilize synchrony between SCN neurons depending on the coupling state of the network (14, 16, 18). However, loss of GABA signaling in all SCN neurons—either pharmacologically or by deletion of the vesicular GABA transporter gene (*Vgat*, also known as *Slc32a1*)—does not cause arrhythmia like the absence of vasoactive intestinal polypeptide (VIP) signaling (20, 21). Cell-type specific genetic deletion studies have recently shed light on this issue, with loss of *Vgat* in VIP- or AVP-expressing cells modifying the properties of entrained and free-running circadian rhythms, respectively, but also failing to induce circadian arrhythmia (22, 23). These studies indicate that GABA signaling from these specific neuronal subpopulations may modulate different SCN network properties but is not necessary for the SCN to sustain circadian rhythmicity. The genetic deletion of *Vgat* restricted to the totality of SCN neurons is currently not feasible and the pan-neuronal silencing of GABA release is lethal. Thus, more intersectional

The authors declare no competing interest.

This article is a PNAS Direct Submission.

[1]To whom correspondence may be addressed. Email: ivanabussi@gmail.com or horaciod@uw.edu.

[2]Present address: Allen Institute for Brain Science, Seattle, WA 98109.

[3]Present address: Laboratorio Interdisciplinario del Tiempo, Escuela de Educación, Universidad de San Andrés/CONICET, Buenos Aires B1644BID, Argentina.

This article contains supporting information online at https://www.pnas.org/lookup/suppl/doi:10.1073/pnas.2314857120/-/DCSupplemental.

Published November 29, 2023.

approaches are needed to fully characterize the GABA function within the SCN.

Neuromedin S (NMS)-expressing SCN neurons are essential for circadian rhythms in behavior and SCN neuronal synchrony (24). Manipulating the circadian period of NMS neurons in mice is sufficient to alter the period of both locomotor activity and SCN rhythms (24). Further, NMS-specific deletion of *Bmal1* or constitutive overexpression of *Per2* to impair the molecular clock function is sufficient to abolish behavioral circadian rhythms and reduce intercellular synchrony in the SCN (24). Finally, blocking the release of synaptic vesicles in NMS^+ neurons likewise abolishes daily rhythms in behavior and attenuates SCN intercellular synchrony (24). Although these results have underscored the role of NMS neurons as critical for the central circadian pacemaker function, NMS itself is not required for daily rhythms in behavior and cellular function (24), suggesting that another signaling factor produced by NMS^+ neurons is necessary for circadian timekeeping. Therefore, we hypothesized that GABA signaling from NMS neurons is necessary to maintain circadian rhythms in behavior and SCN neuronal synchrony.

To test this hypothesis, here we selectively deleted *Vgat* from NMS neurons (*Nms-Vgat*$^{-/-}$ mice) throughout life using a Cre-loxP strategy. As adults, *Nms-Vgat*$^{-/-}$ mice lack intrinsic locomotor activity and sleep-wake rhythms but retain the ability to synchronize to environmental light–dark (LD) cycles via light-induced masking. Consistent with this behavioral phenotype, SCN rhythms of clock gene expression were impaired in *Nms-Vgat*$^{-/-}$ mice. Surprisingly, we found that *Nms-Vgat*$^{-/-}$ mice display reduced VIP immunoreactivity in the SCN without disrupting the number or morphology of SCN VIP neurons. Deletion of *Vgat*, either genetically targeted to the VIP^+ cells in the SCN or virally mediated in the adult SCN, phenocopied reduced VIP immunoreactivity but circadian rhythms in locomotion were intact. Taken together, our results suggest that GABAergic neurotransmission in SCN NMS^+ neurons is necessary for the development and maintenance of circadian rhythms in behavior and central clock function.

Results

***Nms-Vgat*$^{-/-}$ Mice Display Circadian Arrhythmia in Constant Darkness (DD), Fail to Entrain to "Skeleton Photoperiods" (SPs) but Display Masking under 3.5:3.5 LD Cycles.** To evaluate whether GABA transmission is necessary for synchronization, entrainment, and maintenance of coherent circadian rhythms in free-running conditions, we examined circadian rhythms of wheel-running activity in *Vgat*$^{+/+}$, *Nms-Vgat*$^{+/-}$, and *Nms-Vgat*$^{-/-}$ mice in both 12:12 LD and DD conditions (Fig. 1 *A* and *B*). Under LD conditions, mice from all genotypes display nocturnal activity and a reduction of the wheel-running activity during the light phase.

After release into DD, both wild-type control *Vgat*$^{+/+}$ and heterozygous *Nms-Vgat*$^{+/-}$ mice displayed clear rhythms with periods within the circadian range and typical for this mouse strain (23.39 ± 0.11 h for *Vgat*$^{+/+}$ and 23.69 ± 0.07 h for *Nms-Vgat*$^{+/-}$, *SI Appendix*, Table S1). In contrast, 58.8% (20/34) of *Nms-Vgat*$^{-/-}$ mice exhibited arrhythmic locomotor activity patterns in DD (Fig. 1*B*; chi-square periodogram analysis). Visual inspection of actograms indicated that in most cases, this arrhythmia was present from the first day in DD, indicating that the rhythmic behavior under LD conditions resulted from light-induced masking (Fig. 1*A*, left *Nms-Vgat*$^{-/-}$ actogram). The remaining *Nms-Vgat*$^{-/-}$ mice displayed severely disrupted circadian rhythmicity in DD with a period of 23.77 ± 0.15 h (Fig. 1*A*, *Nms-Vgat*$^{-/-}$ right actogram). Disrupted circadian rhythmicity in *Nms-Vgat*$^{-/-}$ mice was further evidenced by less robust rhythms relative to littermate controls, as indicated by the amplitude of the fast-Fourier transform (FFT; Fig. 1*C* and *SI Appendix*, Table S1). Further, rhythmic *Nms-Vgat*$^{-/-}$ mice exhibited an earlier time of activity onset on the first day of DD relative to littermate controls (Fig. 1*D* and *SI Appendix*, Table S1) suggesting that circadian function was also compromised even when *Nms-Vgat*$^{-/-}$ mice were able to maintain behavioral rhythms in DD. Thus, circadian timekeeping in *Nms-Vgat*$^{-/-}$ mice is severely compromised under DD or shows an abnormal phase of entrainment in animals that are not arrhythmic.

To test the integrity of photic entrainment in *Nms-Vgat*$^{-/-}$ mice, we subjected mice of each genotype to a SP (LDLD 1:10:1:12). Under this schedule, mice received two 1-h light pulses framing 10 h of darkness that represent the subjective day in the SP (Fig. 1*E*, top part of the actograms). Because light inhibits locomotor activity in nocturnal rodents, SPs are designed to detect daytime activity and arrhythmic activity patterns masked by light. As expected, activity rhythms in *Vgat*$^{+/+}$ were not altered substantially by the SP, with the majority of activity concentrated during the original subjective night (Fig. 1*E*, left actogram and waveform to the right of each actogram). Heterozygous *Nms-Vgat*$^{+/-}$ mice likewise displayed stably entrained rhythms under the SP (Fig. 1 *E*, *Central*). In contrast, *Nms-Vgat*$^{-/-}$ mice displayed locomotor activity in both daily dark phases, with each 1-h light pulse acutely suppressing activity (Fig. 2 *E*, *Right*). Unlike the phenotypic heterogeneity observed in *Nms-Vgat*$^{-/-}$ mice under DD, nearly every *Nms-Vgat*$^{-/-}$ mouse revealed a lack of true entrainment under the SP. Respectively, *Vgat*$^{+/+}$ and *Nms-Vgat*$^{+/-}$ mice displayed only 11.0 ± 2% and 4.2 ± 1% of activity during the daytime dark phase, compared to 38.8 ± 3% in *Nms-Vgat*$^{-/-}$ mice (Fig. 1*F* and *SI Appendix*, Table S2). These results demonstrate that the locomotor activity pattern displayed by *Nms-Vgat*$^{-/-}$ mice under LD conditions is driven mostly by light suppression of activity.

To further dissect the masking from the circadian response to light, we exposed mice to an ultradian cycle of 7 h (LD 3.5:3.5), which is outside the limits of circadian entrainment (25). As expected, wild-type control *Vgat*$^{+/+}$ and heterozygous *Nms-Vgat*$^{+/-}$ displayed a circadian pattern of locomotor activity, combined with intervals of light-induced masking. In contrast, activity in homozygous *Nms-Vgat*$^{-/-}$ mice was mainly driven by masking effects of light and darkness, with no detectable circadian component (Fig. 1*E*, bottom part of the actogram). Consequently, both *Vgat*$^{+/+}$ and *Nms-Vgat*$^{+/-}$ mice displayed a dominant period in the circadian range while *Nms-Vgat*$^{-/-}$ mice displayed only a peak within the 7-h range (Fig. 1*E*, FFT to the right of each actogram, *SI Appendix*, Table S2). Analysis of the FFT amplitude for the masking and circadian components indicated that the masking response was comparable for all three groups, but *Nms-Vgat*$^{-/-}$ mice displayed reduced amplitude of the circadian component (Fig. 1*G* and *SI Appendix*, Table S2). These results suggest that the behavior of *Nms-Vgat*$^{-/-}$ mice under LD is strongly influenced by the acute effects of light rather than reflecting true entrainment of a functional circadian pacemaker.

In order to confirm the efficiency of the genetic strategy, we performed immunohistochemistry (IHC) against VGAT in brain tissue from behaviorally tested mice, which revealed that VGAT expression was effectively reduced in the dorsal and ventral SCN in both *Nms-Vgat*$^{+/-}$ (30% and 26% respectively), and *Nms-Vgat*$^{-/-}$ (53% and 35%) mice compared to control *Vgat*$^{+/+}$ mice (*SI Appendix*, Fig. S1).

To confirm that our genetic manipulation had the intended effect on GABA release, we conducted two experiments. First, we measured GABA release using the fluorescent GABA sensor iGABASnFR (26). Hypothalamic slices from *Nms-Vgat*$^{-/-}$, *Nms-Vgat*$^{+/-}$, and *Nms-Vgat*$^{+/+}$ (which express Cre recombinase under the control

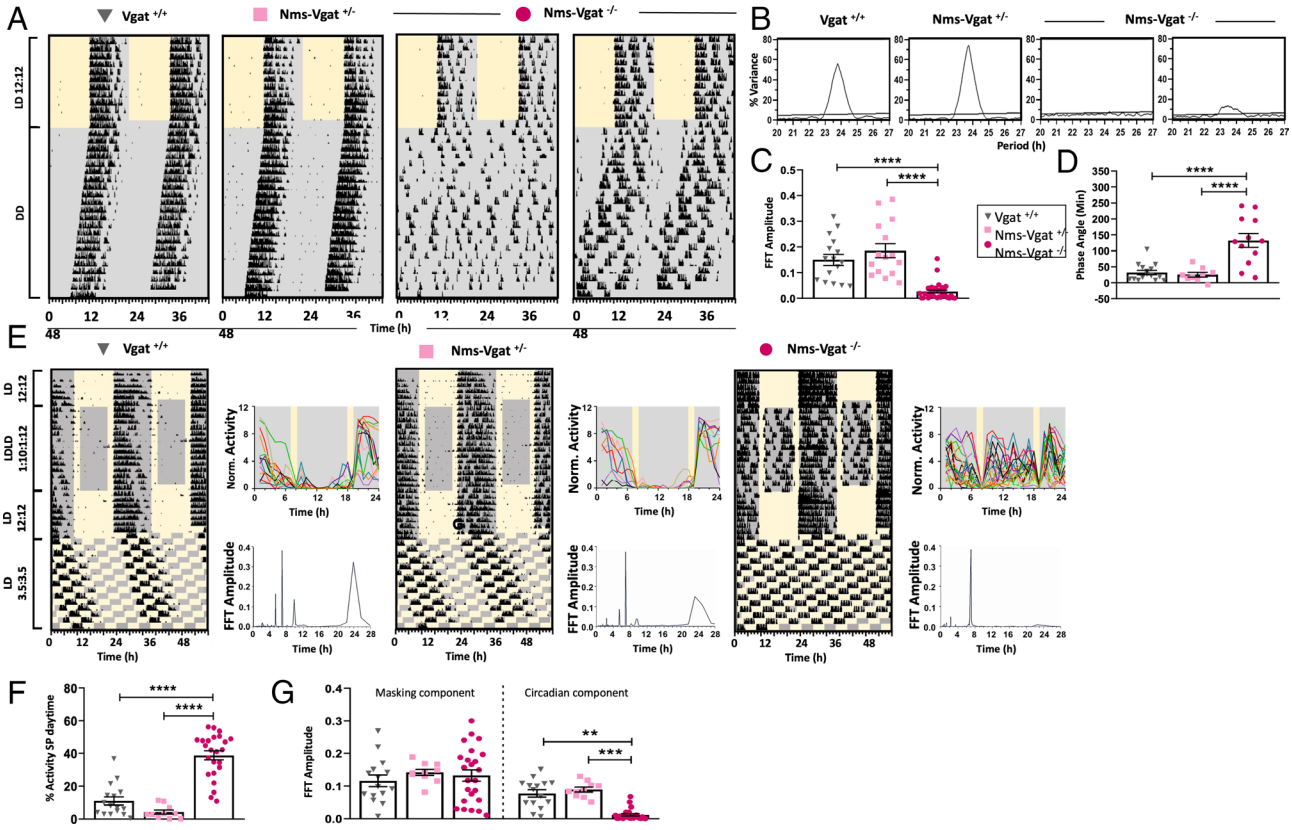

Fig. 1. *Nms-Vgat*$^{-/-}$ mice display arrhythmic locomotor activity in DD, fail to entrain to SPs but display masking under 3.5:3.5 LD cycles. (*A*) Representative double-plotted actograms of *Vgat*$^{+/+}$, *Nms-Vgat*$^{+/-}$, and *Nms-Vgat*$^{-/-}$ mice showing 12 d under a 12:12 LD cycle followed by 21 d in DD. (*B*) Chi-square periodograms during DD of each respective actogram in *A*. Statistical significance is represented by the horizontal line ($P = 0.05$). (*C*) Robustness of the free-running locomotor activity rhythms measured by FFT amplitude in the circadian range (20 to 28 h). One-way ANOVA, $F_{(2,62)} = 12.25$, $P < 0.0001$; *Vgat*$^{+/+}$ n = 16, *Nms-Vgat*$^{+/-}$ n = 15 and *Nms-Vgat*$^{-/-}$ n = 34. (*D*) Time of activity onset on the first day of DD relative to the previous entraining lights-off transition (i.e., phase angle of entrainment). One-way ANOVA, $F_{(2,33)} = 18.45$, $P < 0.0001$; *Vgat*$^{+/+}$ n = 15, *Nms-Vgat*$^{+/-}$ n = 9, *Nms-Vgat*$^{-/-}$ n = 12 (analysis only includes a minority of *Nms-Vgat*$^{-/-}$ mice that were rhythmic). (*E*) Representative double-plotted wheel-running actograms from *Vgat*$^{+/+}$, *Nms-Vgat*$^{+/-}$, and *Nms-Vgat*$^{-/-}$ mice subjected to LD 12:12 for 7 d, a 1:10:1:12 SP for 14 d, LD 12:12 for 7 d, and LD 3.5:3.5 (i.e., T7) for 15 d. Next to each actogram, *Top*: average activity profile illustrating hourly wheel-running levels in individual *Vgat*$^{+/+}$, *Nms-Vgat*$^{+/-}$, and *Nms-Vgat*$^{-/-}$ mice under the 1:10:1:12 SP; *Bottom*: FFT spectra of each mouse displayed in each actogram during the T7 window of the experiment. (*F*) Percentage of wheel revolutions during the daytime dark phase of the SP. One-way ANOVA, $F_{(2, 47)} = 48.40$, $P < 0.0001$; *Vgat*$^{+/+}$ n=16, *Nms-Vgat*$^{+/-}$ n=10, and *Nms-Vgat*$^{-/-}$ n = 24. (*G*) FFT amplitude for 7-h and circadian range (20 to 28 h) for mice subjected to a LD 3.5:3.5 schedule. Two-way ANOVA, Period (~7 h or 20 to 28 h): $F_{(1, 46)} = 45.57$, $P < 0.0001$; Genotype: $F_{(1, 46)} = 4.05$, $P = 0.0239$; Period*Genotype $F_{(2, 46)} = 7.71$ $P = 0.0013$; *Vgat*$^{+/+}$ n = 15, *Nms-Vgat*$^{+/-}$ n = 10, *Nms-Vgat*$^{-/-}$n = 24. Data represented as mean ± SEM. Tukey's post hoc comparisons. $^{**}P < 0.01$, $^{***}P < 0.001$, $^{****}P < 0.0001$.

of the Nms promoter but no loxP sites flanking the *Vgat* gene) mice were infected with an adenoassociated virus (AAV) encoding Cre-dependent iGABASnFR. SCN GABA release showed a genotype-dependent decrease (*SI Appendix*, Fig. S1 *E* and *F*, One-way ANOVA: $F_{(2, 14)} = 5.61$, $P = 0.016$), with *Nms-Vgat*$^{-/-}$ slices showing a decrease of 30.5% relative to *Nms-Vgat*$^{+/+}$ controls. However, the behavioral phenotype of *Nms-Vgat*$^{-/-}$ mice, quantified as the FFT amplitude of circadian wheel-running activity, was not correlated with the GABA release measured ex vivo (Pearson's correlation R = 0.23, $P = 0.55$).

In the second experiment, we conducted whole-cell voltage-clamp recordings of spontaneous $GABA_A$ receptor-mediated postsynaptic currents (sGPSC) from SCN neurons in brain slices from *Nms-Vgat*$^{-/-}$, *Nms-Vgat*$^{+/-}$, and *Nms-Cre*$^{-/-}$-*Vgat*$^{fl/fl}$ mice. We recorded 27, 25, and 29 neurons from each genotype (6 mice per genotype, 10 males and 8 females), respectively. Of these 81 neurons, 16 neurons from 10 different mice (4, 4, and 2 from each genotype, respectively) were discarded as high-frequency outliers (see *Materials and Methods* for details). We used a linear model with mixed effects with genotype, sex, age, and zeitgeber time (ZT) of recording as fixed effects, and mouse as a random effect; only genotype yielded significant effects. Because ZT was the only effect that could change within a mouse (i.e., neurons in the same slice could be recorded at different times) and did not arise as a relevant factor in the previous model, this analysis was further simplified by summarizing the data by mouse. A linear model with the same fixed effects (except for ZT) confirmed that both *Nms-Vgat*$^{-/-}$ and *Nms-Vgat*$^{+/-}$ mice had frequencies that were less than half the frequency of *Vgat*$^{+/+}$ mice (*SI Appendix*, Fig. S1 *G* and *H*; $P = 0.014$ for *Nms-Vgat*$^{-/-}$ and $P = 0.008$ for *Nms-Vgat*$^{+/-}$. *SI Appendix*, Table S9). A similar analysis done for the amplitude of the sGPSC (no outlier values were detected for amplitude) revealed no significant differences between genotypes (*SI Appendix*, Fig. S1*I*; $P = 0.592$ for *Nms-Vgat*$^{-/-}$ and $P = 0.474$ for *Nms-Vgat*$^{+/-}$, *SI Appendix*, Table S9). Together, these results indicate that the deletion of at least one *Vgat* allele within NMS neurons leads to a decrease in the frequency of presynaptic GABA release and sGPSC—confirmed by the lower release detected by the GABA sensor—without affecting the postsynaptic response.

NMS is expressed with high specificity in the SCN but it is also expressed in extra-SCN regions (24), and it remains possible that the severe circadian deficits and *Nms-Vgat*$^{-/-}$ mice result from lack of GABA release from NMS cells in regions other than the SCN. We addressed this possibility by crossing *Nms-Cre* mice with a Cre-dependent *tdTomato* mouse line to label all NMS^+ neurons. Immunostaining for VGAT in brain sections from *Nms-tdTomato*

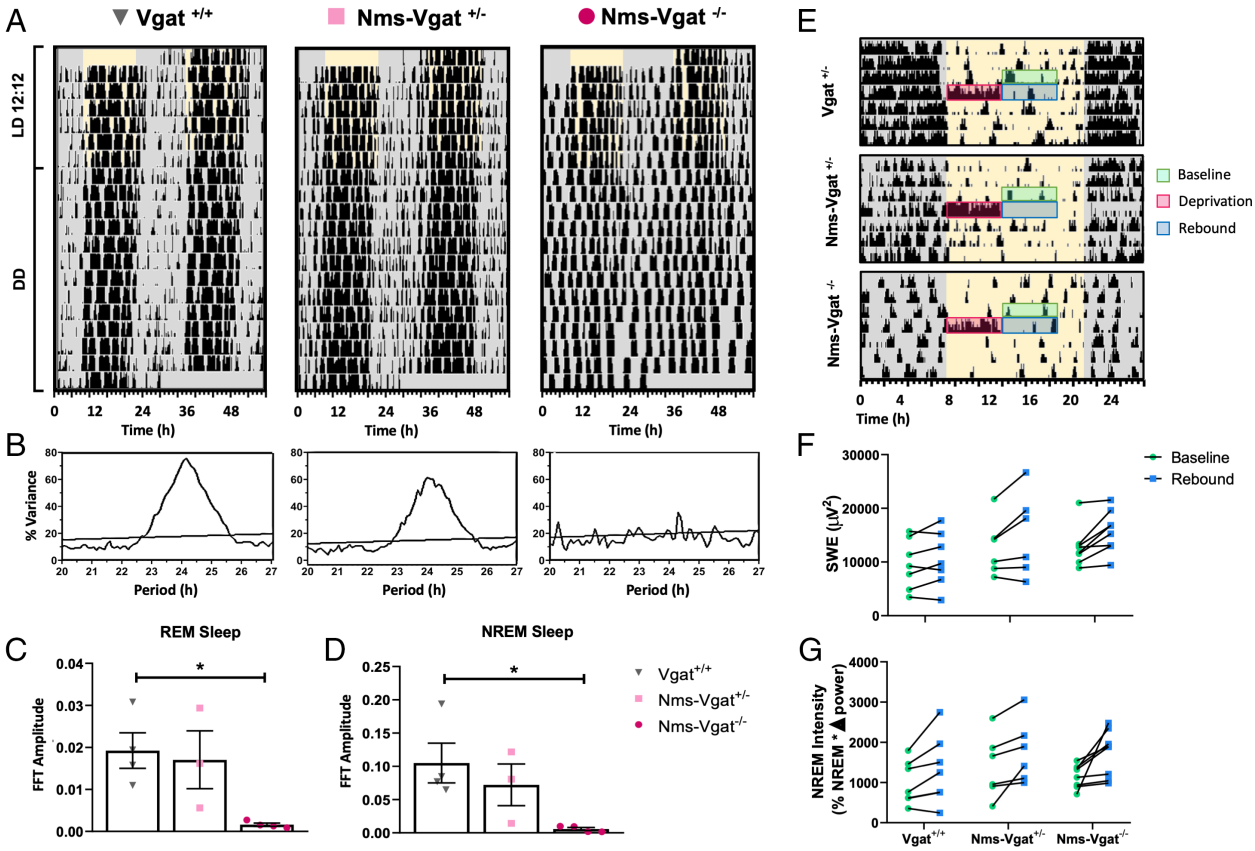

Fig. 2. *Nms-Vgat*$^{-/-}$ mice display circadian arrhythmia in REM and NREM sleep, but normal homeostatic response to sleep deprivation. (*A*) Representative total sleep (REM and NREM sleep) actograms from *Vgat*$^{+/+}$, *Nms-Vgat*$^{+/-}$, and *Nms-Vgat*$^{-/-}$mice subjected to LD 12:12 for 6 d, then released into DD for 12 d. Polysomnographic sleep data are displayed into 10-min bins. (*B*) Chi-square periodograms during DD fraction for actograms in panel (*A*). (*C* and *D*) REM and NREM sleep FFT amplitude within the circadian range under DD. Kruskal–Wallis test, REM sleep: $P = 0.0142$. NREM sleep: $P = 0.0142$; *Vgat*$^{+/+}$ n = 4, *Nms-Vgat*$^{+/-}$ n = 3, *Nms-Vgat*$^{-/-}$ n = 4. Data represented as mean ± SEM. Dunn's post hoc comparisons, $*P < 0.05$. (*E*) Representative home-cage activity actograms from *Vgat*$^{+/+}$, *Nms-Vgat*$^{+/-}$ and *Nms- Vgat*$^{-/-}$ mice in LD subjected to 5-h sleep deprivation. (*F*) Slow wave Energy (SWE) during baseline and rebound. RM ANOVA, Genotype: $F_{(2, 18)} = 1.57$, $P = 0.23$, Time: $F_{(1, 18)} = 19.0$, $P = 0.0004$; Interaction: $F_{(2, 18)} = 1.63$, $P = 0.22$. (*G*) NREM sleep intensity during baseline and rebound. RM ANOVA, Genotype: $F_{(2, 18)} = 0.86$, $P = 0.44$; Time: $F_{(1, 18)} = 18.16$, $P = 0.0005$; Interaction: $F_{(2, 18)} = 0.60$, $P = 0.56$; *Vgat*$^{+/+}$n = 7, *Nms-Vgat*$^{+/-}$ n = 6 and *Nms- Vgat*$^{-/-}$ n = 8.

mice did not reveal any regions expressing both *tdTomato* and VGAT with the exception of the SCN (*SI Appendix*, Fig. S2). Thus, it is unlikely that NMS neurons outside of the SCN were affected by the *Nms-Vgat*$^{-/-}$ targeting strategy.

***Nms-Vgat*$^{-/-}$ Mice Display Arrhythmic Patterns of REM (Rapid-Eye-Movement) and NREM (Non-REM) Sleep in DD, but Normal Homeostatic Response to Sleep Deprivation.** To test the effects of Nms-*specific Vgat* deletion on the circadian regulation of sleep, we recorded sleep polysomnographically under DD. As expected, *Vgat*$^{+/+}$ and *Nms-Vgat*$^{+/-}$ mice displayed circadian rhythms in both REM sleep and NREM sleep, (Fig. 2 *A–D* and *SI Appendix*, Table S3). In contrast, Chi-square periodograms revealed that out of the 4 *Nms-Vgat*$^{-/-}$ mice, 2 were completely arrhythmic for both REM and NREM sleep, one was rhythmic, and another had a weak NREM but no discernible REM sleep rhythm. The severe effect of the *Vgat* deletion on circadian sleep rhythmicity was confirmed by the significantly reduced FFT amplitude in *Nms-Vgat*$^{-/-}$ mice (Fig. 2 *C* and *D* and *SI Appendix*, Table S3). These results complement those for wheel-running rhythms supporting the notion that GABA release by NMS-expressing neurons is also critical for the circadian regulation of sleep.

We next tested whether *Nms*-specific *Vgat* deletion influenced the homeostatic regulation of sleep by depriving mice of sleep from ZT 1-5 (ZT12 being the time of lights-off), then comparing NREM sleep parameters during the 5 h post-deprivation (i.e., the rebound period) to the previous day during the equivalent time (baseline, Fig. 2*E*). During rebound sleep, slow-wave energy (i.e., the cumulative sum of power in the delta frequency band, 0.5 to 4 Hz) was significantly higher relative to baseline across all genotypes (Fig. 2*F* and *SI Appendix*, Table S4). In addition, *Vgat* deletion did not alter NREM intensity, measured as the product of delta power and time spent in NREM sleep per hour (Fig. 2*G* and *SI Appendix*, Table S4). The total duration of NREM sleep, defined by the average percentage of time spent in NREM sleep per hour, was comparable between the two recording windows (*SI Appendix*, Table S4). Given there was no effect of genotype observed for any sleep parameter measured, these results suggest the lack of GABA signaling in NMS^{+} neurons does not affect the homeostatic sleep response in *Nms-Vgat*$^{-/-}$mice.

The SCN Molecular Clock is Impaired in *Nms-Vgat*$^{-/-}$ Mice. To test whether the central SCN clock is impaired in *Nms-Vgat*$^{-/-}$ mice, we investigated SCN molecular rhythms in NMS-expressing neurons using real-time bioluminescence imaging. *Nms-Vgat*$^{+/-}$ and *Nms-Vgat*$^{-/-}$ mice received SCN injections of an AAV encoding Cre-dependent *Per2* promoter-driven luciferase [AAV-P(Per2)-DIO-intron2-dLUC] and their behavior was monitored in DD (Fig. 3*A*). SCN slices were collected 6 to 12 wk after injection for ex vivo imaging of SCN NMS bioluminescence expression (Fig. 3 *B–D*). The overall bioluminescence signal did not differ between *Nms-Vgat*$^{+/-}$ and *Nms-Vgat*$^{-/-}$SCN, with bilateral *Per2*-driven luciferase signal observed in 84% of *Nms-Vgat*$^{+/-}$ SCN slices

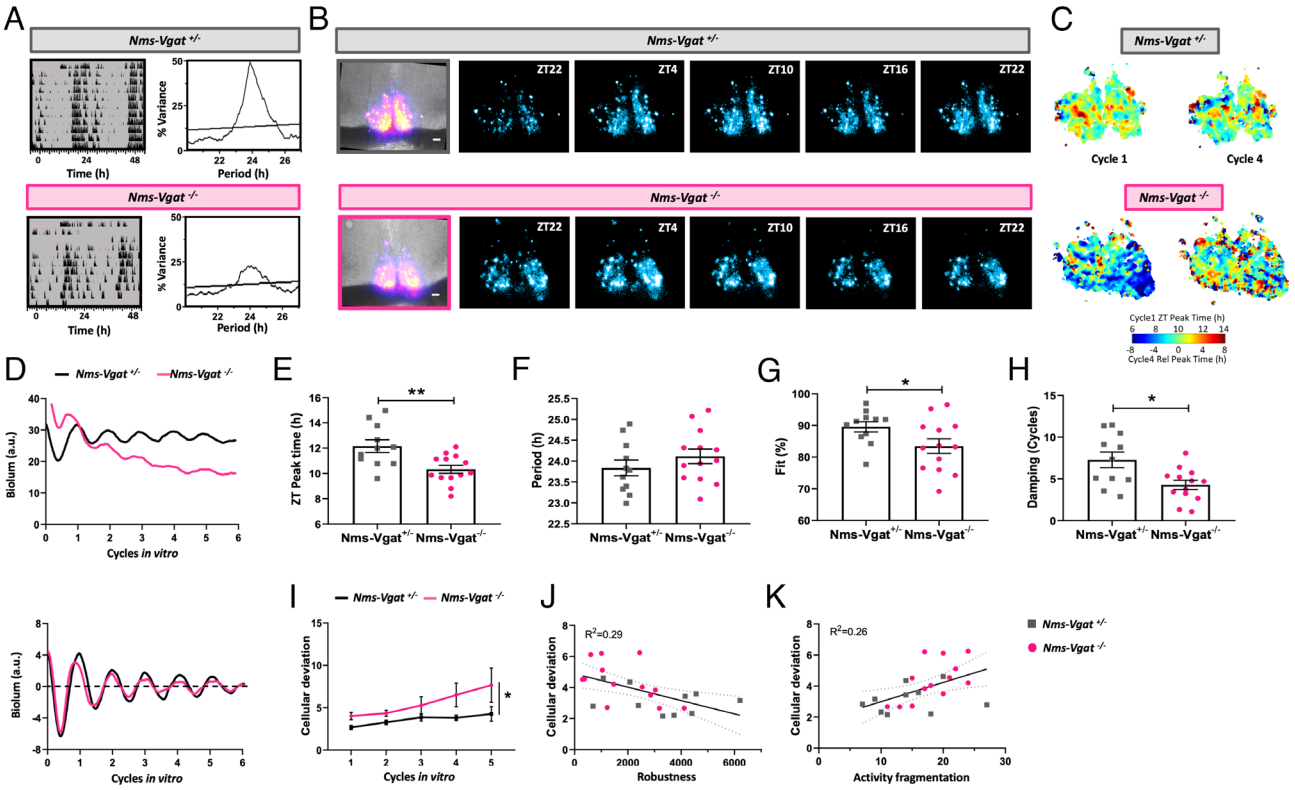

Fig. 3. SCN NMS molecular clock function and intercellular synchronization are impaired in *Nms-Vgat*$^{-/-}$ mice. (*A*) Representative double-plotted wheel-running activity actograms and periodograms from a *Nms-Vgat*$^{+/-}$ and *Nms- Vgat*$^{-/-}$mouse in DD. (*B*) *Per2*-driven luciferase expression from NMS^{+} neurons in a coronal SCN slice from a *Nms-Vgat*$^{+/-}$ and *Nms- Vgat*$^{-/-}$mouse. Leftmost image: 24-h sum superimposed onto bright field image. (Scale bar, 100 μm.) (*Right*) 2-h summed images over the first 24 h of recording. ZT: Zeitgeber Time, ZT12 = projected time of lights-off. (*C*) Color-coded phase maps for the *Nms-Vgat*$^{+/-}$ and *Nms-Vgat*$^{-/-}$ slices in panel (*B*) illustrating SCN organization on the first and fourth cycles in vitro. (*Left*) ZT peak time of *Per2*-driven luciferase rhythms on the first cycle, illustrating earlier peak time in *Nms-Vgat*$^{-/-}$ SCN. (Right) Relative peak time on the fourth cycle, illustrating greater phase desynchrony in *Nms-Vgat*$^{-/-}$ SCN. (*D*) Time series of bioluminescence rhythms during recording for SCN slices in panel (*B*). (*Top*) raw bioluminescence. (*Bottom*) Baseline subtracted. (*E*) ZT peak time in *Nms-Vgat*$^{+/-}$ (n = 11) and *Nms-Vgat*$^{-/-}$ SCN (n = 13). Student's *t* test, ***P* = 0.0068. (*F*) Period length of NMS *Per2* rhythms in *Nms-Vgat*$^{+/-}$ and *Nms-Vgat*$^{-/-}$ SCN. Student's *t* test, *P* = 0.29. (*G*) Goodness of fit calculated for NMS *Per2* rhythms in *Nms-Vgat*$^{+/-}$ and *Nms-Vgat*$^{-/-}$ SCN. Student's *t* test, **P* = 0.0405. (H) Rate of NMS *Per2* rhythm damping in *Nms-Vgat*$^{+/-}$ and *Nms-Vgat*$^{-/-}$ SCN. Student's *t* test, **P* = 0.0147. (*I*) SD of cellular peak times over time in vitro. Repeated measures, *Genotype: *P* = 0.0388; *Time in vitro: *P* = 0.0108; Genotype × Time in vitro: *P* = 0.53. (*J*) Cellular deviation in peak time on the second cycle in vitro correlated with the robustness of the free-running rhythm in vivo. Linear regression Y = –4.31 × 10E-4*X + 4.88; R^2 = 0.29. $F_{(1,21)}$ = 8.78, *P* = 0.0075. Linear regression for each genotype: *Nms-Vgat*$^{+/-}$ R^2 = 0.09, *P* = 0.40; *Nms-Vgat*$^{-/-}$ R^2 = 0.298, *P* = 0.0500. (*K*) Cellular deviation in peak time on the second cycle in vitro correlated with the fragmentation of the free-running locomotor activity rhythm in vivo. Linear regression Y = 0.12*X + 1.76; R^2=0.26. $F_{(1,21)}$= 7.37, *P* = 0.013. Linear regression for each genotype: *Nms-Vgat*$^{+/-}$ R^2 = 0.04, *P* = 0.56; *Nms-Vgat*$^{-/-}$ R^2 = 0.385, *P* = 0.0237. Data represented as mean ± SEM.

and 76% *Nms-Vgat*$^{-/-}$ SCN slices (11/13 and 13/17, respectively). These data suggest that the efficacy of viral transduction of SCN NMS neurons was similar in both genotypes.

SCN NMS *Per2* rhythms differed by genotype in a manner related to phenotype. First, the *Nms-Vgat*$^{-/-}$ SCN displayed an earlier time of peak gene expression on the first cycle ex vivo compared to the *Nms-Vgat*$^{+/-}$ SCN (Fig. 3 *C* and *E* and *SI Appendix*, Table S5). This result is consistent with the advanced phase of locomotor rhythms observed in *Nms-Vgat*$^{-/-}$ mice after release into DD (c.f., Fig. 1*D*), suggesting the *Nms-Vgat*$^{-/-}$ SCN has an advanced phase in vivo. Further, SCN period did not differ by genotype (Fig. 3*F* and *SI Appendix*, Table S5), but the quality of rhythms was lower in the *Nms-Vgat*$^{-/-}$ SCN (Fig. 3 *G* and *H* and *SI Appendix*, Fig. S3). Specifically, the goodness of the cosinor fit for *Per2*-driven luciferase rhythms was lower in *Nms-Vgat*$^{-/-}$ SCN than in *Nms-Vgat*$^{+/-}$ SCN (Fig. 3*G* and *SI Appendix*, Table S5). In addition, *Per2*-driven luciferase rhythms damped faster in *Nms-Vgat*$^{-/-}$ SCN than in *Nms-Vgat*$^{+/-}$ SCN (Fig. 3*H* and *SI Appendix*, Table S5). Last, the SD of cellular peak times increased more in *Nms-Vgat*$^{-/-}$ SCN neurons than *Nms-Vgat*$^{+/-}$ SCN neurons (Fig. 3 *C* and *I* and *SI Appendix*, Table S5). Notably, cellular deviation on the second cycle ex vivo was correlated with the robustness and consolidation of locomotor rhythms in vivo. Interestingly, when separated by genotype, only *Nms-Vgat*$^{-/-}$ mice showed a statistically significant correlation between cellular deviation and behavioral impairment (Fig. 3 *J* and *K*). These results indicate that loss of GABA release from NMS neurons impairs molecular clock function and intercellular synchronization. Importantly, changes in the phase, quality, and synchrony of SCN NMS cellular rhythms correspond to the changes observed at the behavioral level.

SCN VIPergic Immunoreactivity in Axonal Terminals is Reduced in *Nms-Vgat*$^{-/-}$ Mice. We next tested whether NMS-driven *Vgat* deletion disrupts SCN neurochemistry. The SCN is roughly divided into two subregions: the ventral core that contains neurons that express the neuropeptide VIP and the dorsal shell that contains neurons that express AVP (8). Both neuropeptides serve as SCN coupling factors and output signals (reviewed in ref. 27). VIP fibers make dense connections with SCN and extra-SCN neurons, whereas AVP fibers project mainly to extra-SCN targets. NMS itself is not needed to sustain circadian rhythms but NMS^{+} neurons include virtually all VIP^{+} and AVP^{+} neurons (24). To test whether the *Vgat* deletion in NMS^{+} cells affects VIP or AVP, we performed double-label IHC for these neuropeptides in *Vgat*$^{+/+}$, *Nms-Vgat*$^{+/-}$, and *Nms-Vgat*$^{-/-}$ SCN (Fig. 4*A*). The number of AVP^{+} and VIP^{+} neuronal cell bodies did not differ

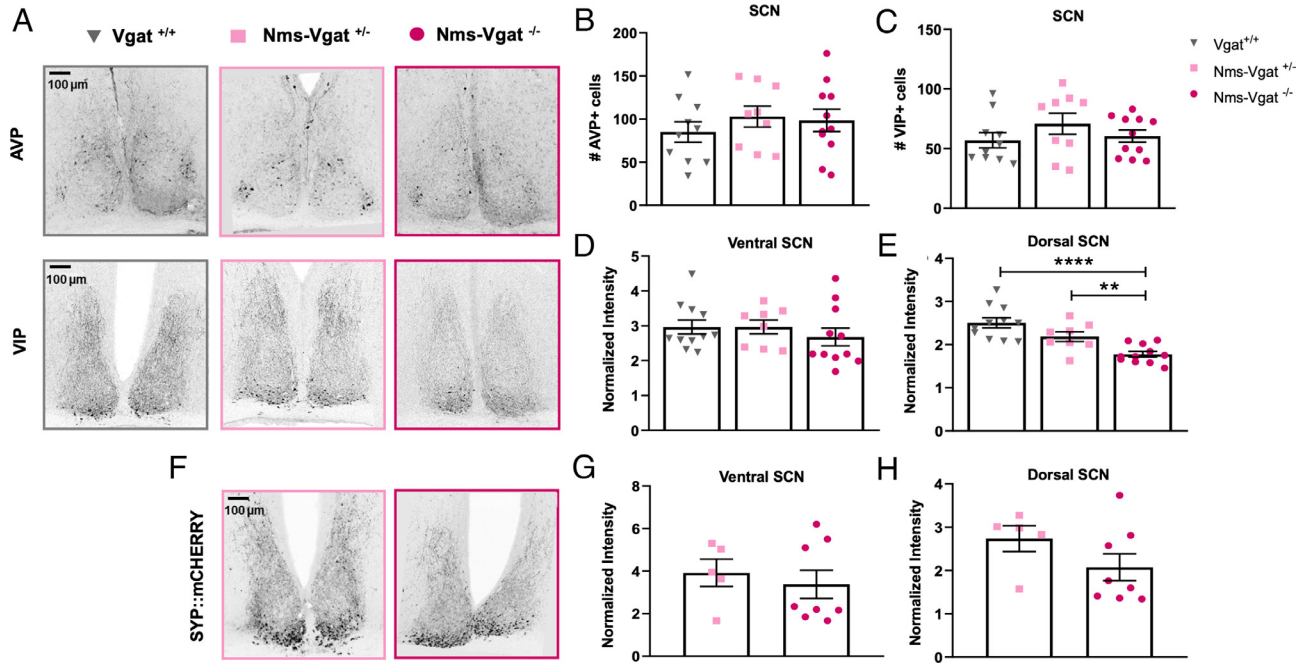

Fig. 4. SCN VIPergic fiber immunoreactivity is reduced in *Nms-Vgat*$^{-/-}$ mice. (*A*) Representative images of AVP and VIP immunostaining in the SCN of *Vgat*$^{+/+}$, *Nms-Vgat*$^{+/-}$, and *Nms-Vgat*$^{-/-}$ mice. (*B*) Number of AVP+ cells in the SCN for all three groups. One-way ANOVA, $F_{(2, 27)} = 0.54$, $P = 0.59$; *Vgat*$^{+/+}$ n = 10, *Nms-Vgat*$^{+/-}$ n = 9, *Nms-Vgat*$^{-/-}$n = 11. (*C*) Number of VIP^{+} cells in the SCN for all three groups. One-way ANOVA, $F_{(2, 27)} = 1.09$, $P = 0.35$; *Vgat*$^{+/+}$ n = 10, *Nms-Vgat*$^{+/-}$ n = 8, *Nms-Vgat*$^{-/-}$ n = 11. (*D* and *E*) Normalized VIP intensity in the ventral (*D*) and dorsal SCN (*E*). Ventral SCN: One-way ANOVA, $F_{(2, 27)} = 1.07$, $P = 0.36$; Dorsal SCN: One-way ANOVA, $F_{(2, 27)} = 14.25$, $P < 0.0001$; *Vgat*$^{+/+}$ n = 10, *Nms-Vgat*$^{+/-}$ n = 9, *Nms-Vgat*$^{-/-}$n = 11). (*F*) Representative images of Syp::mCherry in the SCN of *Nms-Vgat*$^{+/}$ and *Nms-Vgat*$^{-/-}$ mice. (*G* and *H*) Normalized Syp::mCherry intensity in the ventral (*G*) and dorsal SCN (*H*). Ventral SCN: Mann-Whitney test, $P = 0.94$; Dorsal SCN: Mann-Whitney test, $P = 0.13$; *Nms-Vgat*$^{+/-}$ n = 5, and *Nms-Vgat*$^{-/-}$ n = 8. Data represented as mean ± SEM. Tukey's post hoc comparisons, $^{**}P < 0.01$, $^{****}P < 0.0001$.

across genotypes (Fig. 4 *B* and *C* and *SI Appendix*, Table S6). Furthermore, the intensity of VIP immunoreactivity did not differ across genotypes in the ventral SCN (Fig. 4*D* and *SI Appendix*, Table S6). In contrast, the intensity of VIP immunoreactivity in the dorsal SCN was reduced in *Nms-Vgat*$^{-/-}$ mice compared to *Vgat*$^{+/+}$ and *Nms-Vgat*$^{+/-}$ mice (Fig. 4*E* and *SI Appendix*, Table S6).

Decreased VIPergic immunostaining in the dorsal SCN of *Nms-Vgat*$^{-/-}$ mice could reflect impaired VIP transport or a defect in VIP axonal terminals themselves. To address this question, we injected the bilateral SCN of *Nms-Vgat*$^{+/-}$ and *Nms-Vgat*$^{-/-}$ mice with a Cre-dependent AAV expressing *Synaptophysin::mCherry* (*Syp::mCherry*) to assess the effect of *Vgat* deletion on presynaptic fibers from NMS^{+} neurons expressing Cre recombinase. Qualitatively, the fibers looked comparable in both groups of mice (Fig. 4*F*). Quantitatively, genotype did not influence the fluorescence intensity of the fused *Syp::mCherry* either in the ventral or the dorsal SCN (Fig. 4 *G* and *H* and *SI Appendix*, Table S6). Taken together, our results suggest that *Vgat* deletion in NMS^{+} cells reduces VIP expression in axonal terminals without interfering with axonal and synaptic development.

***Vip-Vgat*$^{-/-}$ Mice Display Decreased SCN VIP Expression in the SCN But Not Behavioral Arrhythmia.** Most SCN VIP neurons are NMS^{+} (24, 28), and VIP signaling is critical for SCN function (29, 30). Thus, the severe circadian deficits observed in *Nms-Vgat*$^{-/-}$mice could be caused by the lack of GABA release specifically from VIPergic neurons. To test this hypothesis, we generated VIP-specific *Vgat*-knockout (KO) mice by crossing *Vip-Cre* mice with *Vgat*$^{fl/fl}$ mice and examined wheel-running rhythms in *Vgat*$^{+/+}$, *Vip-Vgat*$^{+/-}$, and *Vip-Vgat*$^{-/-}$ mice under different lighting conditions (*SI Appendix*, Figs. S4 and S5 and Fig. 5*A*). This approach was previously used by Todd et al. (22), who found that locomotor activity rhythms were not altered in LD and DD in *Vip-Vgat*$^{-/-}$ mice. However, we considered it critical to replicate this experiment and do a more extensive characterization of locomotor activity rhythms under the same laboratory conditions under which *Nms-Vgat*$^{-/-}$ mice displayed circadian arrhythmia. Mice in all three genotypes, including *Vip-Vgat*$^{-/-}$, showed nocturnal rhythms under both the LD cycle and the SP (*SI Appendix*, Fig. S5). Under DD, all mice displayed circadian rhythms within the typical range of periods (Fig. 5*B* and *SI Appendix*, Table S7). Further, FFT amplitude of the dominant period did not differ by genotype (Fig. 5*C* and *SI Appendix*, Table S7), indicating similar rhythm robustness. Relative to *Vgat*$^{+/+}$ littermates, both *Vip-Vgat*$^{+/-}$ and *Vip-Vgat*$^{-/-}$ displayed reduced VIP expression in the ventral SCN. Importantly, the intensity of the VIP immunostaining in the dorsal SCN showed a linear relationship with the number of *Vgat* copies, and was less intense in *Vip-Vgat*$^{-/-}$mice (Fig. 5 *D*–*F* and *SI Appendix*, Table S7). Thus, the loss of GABAergic release from VIP neurons reduced SCN VIP expression but did not lead to loss of behavioral circadian rhythmicity. This result indicates that the diminished VIP immunoreactivity observed in *Nms-Vgat*$^{-/-}$ mice is not sufficient to explain their circadian arrhythmia.

***Vgat* KO in Adult SCN Neurons Decreases SCN VIP Expression but Mildly Affects Circadian Rhythms.** To test whether GABAergic transmission in *Nms*-expressing neurons is critical for adult SCN function and/or SCN network development (11), we deleted *Vgat* by injecting a *Gfp-Cre*-expressing AAV into the SCN of *Vgat*$^{fl/fl}$ adult mice and tested for changes in free-running locomotor activity rhythms in DD (Fig. 5*G*). Following histological identification of SCN *Vgat* deletion (Fig. 5*H*), behavioral data were segregated based on whether the injection was on- or off-target (*SCN-Vgat*$^{-/-}$ and *SCN-Vgat*$^{+/+}$ mice, respectively). Mice with unilateral SCN injections or injections that did not fill the extent of both nuclei were excluded from the analyses. Viral-mediated SCN *Vgat* deletion

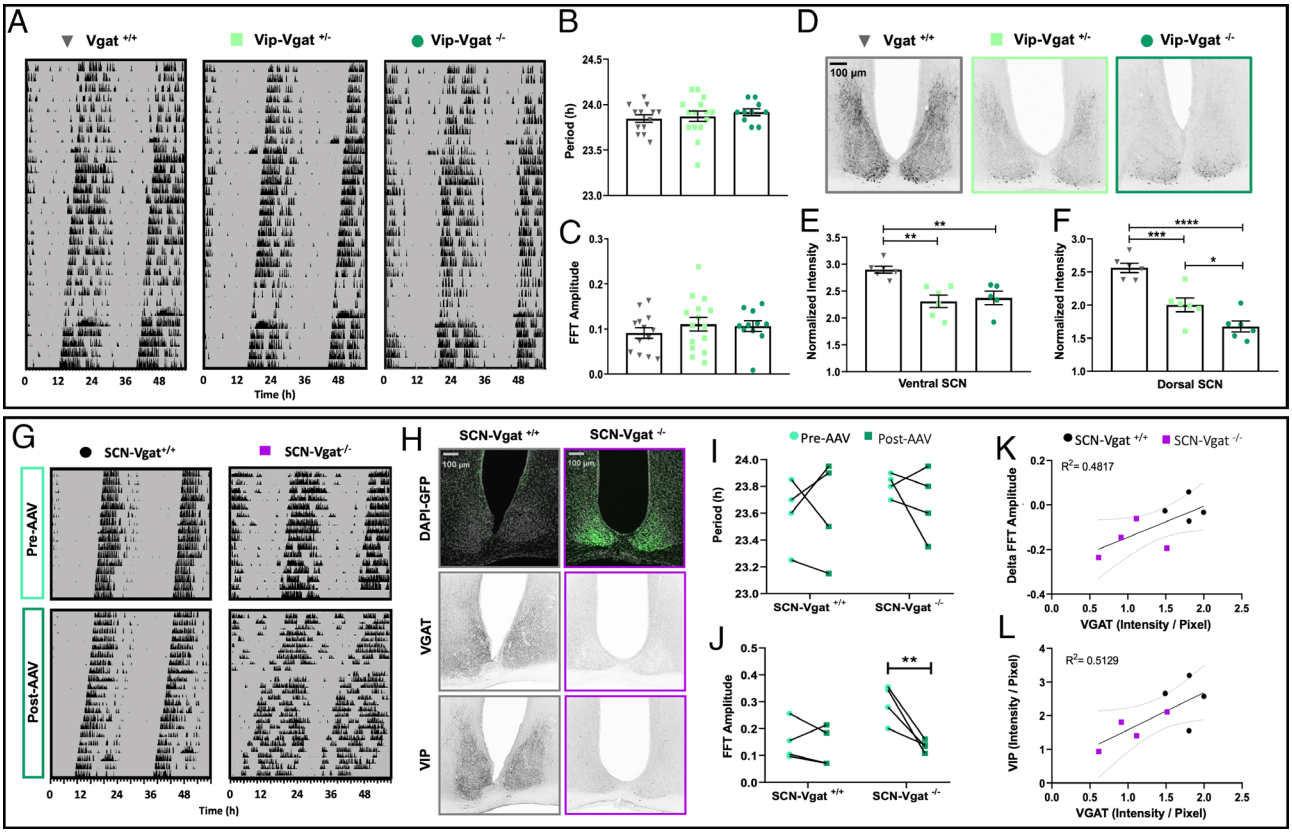

Fig. 5. Targeted deletion of *Vgat* genetically to *Vip* neurons or virally to the adult SCN impairs VIP expression but mildly affects circadian rhythmicity. (*A*) Representative double-plotted wheel-running actograms of *Vgat*$^{+/+}$, *Vip-Vgat*$^{+/-}$, and *Vip-Vgat*$^{-/-}$ mice in DD. (*B*) Free running periods of *Vgat*$^{+/+}$, *Vip-Vgat*$^{+/-}$, and *Vip-Vgat*$^{-/-}$mice. One-way ANOVA, $F_{(2,35)} = 0.46$, $P = 0.63$; *Vgat*$^{+/+}$ n = 13, *Vip-Vgat*$^{+/-}$ n = 15, and *Vip-Vgat*$^{-/-}$n = 11. (*C*) FFT amplitude of *Vgat*$^{+/+}$, *Vip-Vgat*$^{+/-}$, and *Vip-Vgat*$^{-/-}$mice. One-way ANOVA, $F_{(2,36)} = 0.59$, $P = 0.56$. *Vgat*$^{+/+}$ n = 13, *Vip-Vgat*$^{+/-}$ n = 15, and *Vip-Vgat*$^{-/-}$n = 11. (*D*) Representative images of VIP protein expression in the SCN of *Vgat*$^{+/+}$, *Vip-Vgat*$^{+/-}$, and *Vip-Vgat*$^{-/-}$ mice. (*E* and *F*) Normalized VIP immunohistochemical intensity in the ventral (*E*) and dorsal SCN (*F*) of *Vgat*$^{+/+}$, *Vip-Vgat*$^{+/-}$, and *Vip-Vgat*$^{-/-}$mice. One-way ANOVA: Ventral SCN $F_{(2,14)} = 10.2$, $P = 0.0018$; Dorsal SCN $F_{(2,15)} = 26.99$, $P < 0.0001$; *Vgat*$^{+/+}$ n = 6, *Vip-Vgat*$^{+/-}$ n = 6, and *Vip-Vgat*$^{-/-}$ n = 6. (*G*) Representative double-plotted actograms of *SCN-Vgat*$^{+/+}$and *SCN-Vgat*$^{-/-}$ mice in DD before and after AAV-mediated *Vgat* deletion. (*H*) Representative images of GFP, VGAT, and VIP IHC in SCN-*Vgat*$^{+/+}$ and SCN-*Vgat*$^{-/-}$mice. (*I*) Period in DD of SCN-*Vgat*$^{+/+}$ and SCN-*Vgat*$^{-/-}$mice before and after AAV-mediated *Vgat* deletion. RM ANOVA: Time $F_{(1,6)} = 0.298$, $P = 0.60$; Treatment $F_{(1,6)} = 0.704$, $P = 0.43$; Interaction $F_{(1,6)} = 0.62$; $P = 0.46$. (*J*) FFT amplitude of SCN-*Vgat*$^{+/+}$ and SCN-*Vgat*$^{-/-}$mice in DD before and after AAV-mediated *Vgat* deletion. RM ANOVA: Time $F_{(1,6)} = 14.50$, $P = 0.0089$; Treatment $F_{(1,6)} = 3.34$, $P = 0.1176$; Interaction $F_{(1,6)} = 9.18$ $P = 0.0231$. Bonferroni's post-hoc comparisons $^{**}P = 0.0058$; SCN-*Vgat*$^{+/+}$ n = 4, SCN-*Vgat*$^{-/-}$n = 4. (*K*) Correlation between VGAT intensity in the SCN and FFT Amplitude of SCN-*Vgat*$^{+/+}$ and SCN-*Vgat*$^{-/-}$mice. Linear regression equation: Y = 0.14*X – 0.28; $R^2 = 0.48$. $F_{(1,6)} = 5.58$, $P = 0.06$. (*L*) Correlation between VIP and VGAT immunohistochemical intensity in the SCN of SCN-*Vgat*$^{+/+}$ and SCN-*Vgat*$^{-/-}$mice. Linear regression equation: Y = 1.11*X + 0.47; $R^2 = 0.51$. $F_{(1,6)} = 6.32$, $P = 0.0457$. Data represented as mean ± SEM. Tukey's post hoc comparisons, $^{*}P < 0.05$, $^{**}P < 0.01$, $^{***}P < 0.001$, $^{****}P < 0.0001$.

did not abolish free-running rhythms or change their period but did reduce their FFT amplitude (Fig. 5 *I* and *J* and *SI Appendix*, Table S8). These behavioral results are consistent with the findings by Ono et al. (21). There was a trend for the intensity of VGAT immunoreactivity to decrease in the SCN of SCN-*Vgat*$^{-/-}$ mice, but the difference was not statistically significant (*SI Appendix*, Table S8). Of note, our viral injections only target the deletion of *Vgat* within SCN neurons, but the VGAT expression remains in GABAergic terminals within SCN afferent projections, which impairs our ability to accurately quantify the proportion of cells in which *Vgat* was effectively deleted by the viral injection. Despite this limitation and the general variability that is inherent to viral injections depending on injection location and viral expression, we observed a trend for a correlation between VGAT intensity and the delta FFT amplitude (Fig. 5*K* and *SI Appendix*, Table S8). In this plot, the genotypes are well segregated, suggesting that the decrease in locomotor activity robustness in SCN-*Vgat*$^{-/-}$ mice may be explained by the reduction of *Vgat* expression in the SCN. Interestingly, VGAT and VIP levels were positively correlated (Fig. 5*L* and *SI Appendix*, Table S8). Although this result is based on immunoreactivity and does not imply changes in VIP release, it further supports the notion that the deletion of *Vgat* affects VIP transport or processing in neuronal fibers. Taken together, these results indicate that although targeting the deletion of *Vgat* to the adult SCN does not abolish circadian rhythms, it causes a reduction of VIP expression in the SCN.

Discussion

In the present study, we show that deletion of the gene coding for the vesicular GABA transporter, VGAT, from NMS-expressing neurons leads to a severe disruption of circadian rhythmicity. The majority of the *Nms-Vgat*$^{-/-}$ mice show arrhythmic circadian locomotor activity and sleep and all of them show responses to light that reveal a lack of a functional central circadian pacemaker. In contrast, deletion of *Vgat* from VIP-expressing neurons or deletion of *Vgat* targeted to the whole adult SCN has relatively mild effects on circadian rhythmicity. Our results support the idea that intact GABAergic transmission within the SCN, throughout or at specific stages of development, is critical to sustain circadian rhythmicity in the adult.

Although GABA is the most abundant neurotransmitter in the SCN, its role in modulating and coordinating circadian rhythms has yet to be fully unraveled. Initial studies in the adult SCN of both rats and mice suggested that GABA had an interneuron coupling role. Application of GABA to dispersed mouse SCN neurons

had the ability to phase shift their circadian firing rhythm and synchronize them to a common phase (12). This result was consistent with evidence that indicated that GABA could play a role in resynchronizing the core and shell subdivisions of the SCN (13, 19). In contrast, studies in the mouse showed that the long-term blockade of GABAergic transmission in SCN slices had negligible effects on the ability of SCN cells to display coherent circadian rhythms in PER2::LUC expression (20). Later studies suggested that GABA could, in fact, oppose cell-to-cell circadian synchrony (18). These apparently contradicting findings became better reconciled under a current model, which proposes that the role of GABA diverges depending on the preexisting state of synchrony of the SCN neuronal network, on its type of release, and on whether it excites or inhibits the postsynaptic neurons. GABA signaling increases synchrony when subpopulations of neurons are out of phase but can have a phase-repelling effect when the network is tightly synchronized (14–16). Further, synaptically released GABA activates phasic $GABA_A$ receptor-mediated currents, and GABA diffusing out of the synapse activates a tonic current mediated by extrasynaptic $GABA_A$ receptors (31). Mathematical modeling shows that only the tonic current can shift the molecular clock of target neurons (17). Finally, the same modeling reveals that tonic GABA current only shifts the circadian phase of target neurons on which GABA is excitatory, which depends on the chloride equilibrium of the postsynaptic neuron. These model predictions are in line with the GABA-mediated resynchronization of SCN subregions after exposure to long photoperiods, which depends on excitatory effects of GABA and relies on the photoperiod regulation of expression of chloride channels (15).

Even as the role of GABA within the central circadian clock is starting to come to light, none of the above results suggests that GABAergic transmission within the SCN is essential for the neuronal network to sustain overt circadian rhythms. This lack of evidence is not a limitation of pharmacological means to block GABAergic transmission because recent studies that have targeted the deletion of *Vgat* to the adult SCN using viral injections [(21) and our study] and its genetic deletion to AVPergic or VIPergic neurons using specific Cre drivers have also shown relatively mild disruptions of locomotor activity rhythms and normal rhythms of expression of PER2::LUC in the SCN (22, 23). In this regard, we propose that the severe disruption of circadian rhythmicity displayed by *Nms-Vgat*$^{-/-}$ mice reveals a critical role for GABA release within NMS-expressing neurons in the SCN throughout development. Even though *Nms* as a driver targets only 40% of the cells in the SCN (24), it is expressed in a more heterogeneous group of cells than the drivers used in the above studies.

An alternative hypothesis to our results is that synaptic GABA release from NMS neurons is critical to control distal synaptic targets that sustain behavioral rhythms. We do not favor this interpretation for two reasons. First, locomotor activity rhythms, which are severely impaired in *Nms-Vgat*$^{-/-}$ mice, do not rely on synaptically released transmitters from the SCN to its downstream targets (32). Second, as stated above, the deletion of the vesicular GABA transporter in the adult SCN has only mild effects on behavioral circadian rhythms. Finally, the possibility exists that the adult targeting of *Vgat* deletion to the entire SCN could remove GABAergic transmission in cells where GABA has opposing effects, compensating for the effect of the mutation. This alternative hypothesis could be addressed in future studies with inducible KO strategies targeting NMS neurons in adult mice.

Our results contrast with all previous attempts to interfere with SCN GABAergic transmission genetically or pharmacologically, which have shown that GABA neurotransmission in the adult SCN regulates the pattern of SCN neuronal firing and refines the output of the circadian clock but is not critical for the central clock to sustain circadian outputs (11). One possible explanation for this discrepancy could be that the extreme circadian phenotype we observe in *Nms-Vgat*$^{-/-}$ mice is due to the lack of *Vgat* expression in extra-SCN NMS-expressing neurons. We believe this is unlikely for several reasons. First, we show that VGAT is not expressed in NMS-expressing neuronal cell bodies within regions that regulate sleep and circadian rhythms outside of the SCN (*SI Appendix*, Fig. S2), although we cannot discard expression in the axons of these neurons. Second, deletion of *Vgat* from NMS^{+} neurons impairs SCN function as evidenced by the reduction of GABA release and of postsynaptic GABAergic current frequency in SCN neurons, as well as by the impairment of both molecular clock function and intercellular synchronization within the SCN. Third, to the extent of our knowledge, there are no gene deletions that lead to circadian arrhythmia unless they target genes with a critical role in SCN function, such as the deletion of the clock gene *Bmal1* or the *Vip* gene. Fourth, whereas our manipulation led to a lack of circadian regulation of behavior and sleep, it left intact the homeostatic regulation sleep and the masking of locomotor activity by light. Of note, acute masking effects by light are mediated by circuits that are independent of retinal projections to the SCN (33). Together, the lack of effects of the deletion of *Vgat* from NMS neurons on homeostatic regulation of sleep and light masking argues against broad-spectrum effects of the deletion strategy that could affect other GABA-dependent functions, and instead supports a circadian pacemaker-specific effect.

Kingsbury et al. (34) used an SCN network model in which the excitatory effect of VIP transmission within the SCN is mathematically simulated in conjunction with the inhibitory effect of GABA. Interestingly, the model predicts a synchronized neuronal network at varying levels of VIP transmission only when this transmission is matched by similar changes in GABA transmission. Importantly, the transmitters are not modeled to exert opposing actions on each neuron but, instead, to change network properties that can achieve phase synchrony among neurons even in the presence of different firing rates and levels of clock gene expression. This model accurately predicts the results we showed for VIP immunoreactivity in the SCN of *Nms-Vgat*$^{-/-}$, where the lack of GABA signaling caused a dramatic decrease in VIP content. Given that VIP has been shown to be an essential neurotransmitter for the SCN neuronal network to operate synchronously and sustain overt circadian rhythms, it is reasonable to think that our results could be explained in part by the lack of VIP immunoreactivity in the SCN (29, 35). In support of this interpretation, we found that *Nms-Vgat*$^{-/-}$ mice show reduced axonal VIP immunoreactivity. However, we also found a similar, reduced axonal VIP immunoreactivity in animals in which the deletion of *Vgat* was genetically targeted to VIP-expressing neurons or in animals in which the deletion was induced through a Cre-expressing virus in the adult, but neither manipulation led to circadian arrhythmicity as the one displayed by *Nms-Vgat*$^{-/-}$ mice. Together, these results suggest that the lack of VIP in axonal terminals is likely an epiphenomenon and not causally involved in the arrhythmic phenotype of *Nms-Vgat*$^{-/-}$ mice. Importantly, *Nms*-expressing neurons include neurons expressing VIP as well as neurons expressing AVP and other neurons that are critical for normal SCN function (24). Importantly, AVP neurons are not critical to sustain behavioral rhythmicity (22). However, our results suggest that GABA release by non-VIPergic or, alternatively, by a combination of both VIPergic and non-VIPergic neurons during a developmental time window is critical for normal adult

SCN function. This role of GABA in circuit assembly has been recently suggested using an inducible KO for *Vgat* (36).

A role for GABAergic transmission in SCN circuit development has been suggested by recent studies in fetal SCN. SCN slices from global *Vgat*$^{-/-}$ mouse fetuses display normal PER2::LUC rhythms but severely disrupted circadian rhythms in firing and intracellular Ca^{++} oscillations (21). These results are consistent with the fact that SCN cells can display rhythms of PER2 expression early in development, even before critical neurotransmitters are expressed (37). Together, these findings suggest that synchronous intercellular clock-gene expression in the SCN is not sufficient for a functional tissue pacemaker. Our finding that *Per2* circadian transcription in the SCN of *Nms-Vgat*$^{-/-}$ was disrupted but not as severely disrupted as the SCN circadian outputs of sleep and locomotor activity rhythms is consistent with this interpretation. Alternatively, the coherence of clock gene expression within the SCN of *Nms-Vgat*$^{-/-}$ mice in vivo may be more disrupted than ex vivo due to enhanced dissection-induced resetting, a phenomenon that has been observed when arrhythmia is induced by constant light (38, 39). Thus, the lack of GABA signaling from NMS neurons may cause the SCN network to be more susceptible to dissection-induced resetting and/or reconsolidation of cellular rhythms, which damp rapidly over time in culture due to impaired intrinsic timekeeping.

Our results and those in global *Vgat* KOs (21) also suggest that GABAergic transmission during fetal life may be critical to establish key network properties of a functional central pacemaker that are manifested in the adult. Notably, while the deletion of *Vgat* from NMS neurons led to a decrease in the release of GABA and in the frequency of postsynaptic GABA currents in the adult SCN, the impairment of adult circadian behavior was correlated with the level of impairment in the molecular clock but not with the level of impairment of GABA release. This finding further supports that the circadian arrhythmia in *Nms-Vgat*$^{-/-}$ mice is due to the lack of GABA release throughout development and not in the adult.

In conclusion, our study suggests that GABA release, a defining feature of SCN neurons, is critical for the central clock to sustain circadian rhythmicity because of a critical role of the neurotransmitter in the developmental wiring of the SCN rather than of its role in SCN interneuron communication in the adult.

Materials and Methods

Animals. *Vgat*$^{fl/fl}$ mice possess loxP sites flanking exon 2 of both alleles of the *Slc32a1* gene (Slc32a1^{tm1Lowl}/J, Stock No: 012897, Jackson Laboratories). *Vgat*$^{fl/fl}$ mice were crossed to *Nms-Cre* mice [(24); C57BL/6-Tg(*Nms-iCre*)20Ywa, Stock No: 027205, Jackson Laboratories], to generate *Nms-Cre*$^{+/-}$;*Vgat*$^{fl/fl}$ (*Nms-Vgat*$^{-/-}$), *Nms-Cre*$^{+/-}$;*Vgat*$^{fl/+}$ (*Nms-Vgat*$^{+/-}$), *Nms-Cre*$^{-/-}$;*Vgat*$^{fl/fl}$ (*Vgat*$^{+/+}$) and *Nms-Cre*$^{+/-}$;*Vgat*$^{+/+}$ (*Nms-Vgat*$^{+/+}$) mice.

Vgat$^{fl/fl}$ mice were also crossed to *Vip-IRES-Cre* mice, expressing the Cre recombinase under the control of VIP promoter (*Vip*$^{tm1(cre)Zjh}$/J, Stock No: 010908, Jackson Laboratories) to generate *Vip-Cre*$^{+/-}$;*Vgat*$^{fl/fl}$ (*Vip-Vgat*$^{-/-}$), *Vip-Cre*$^{+/-}$;*Vgat*$^{fl/+}$ (*Vip-Vgat*$^{+/-}$) and *Vip-Cre*$^{-/-}$;*Vgat*$^{fl/+}$ (*Vgat*$^{+/+}$) mice.

Nms-Cre mice were also crossed to Cre-dependent *tdTomato*-expressing mice (*B6.Cg-Gt(ROSA)26Sortm14(CAG-tdTomato)Hze/J*, Stock No: 007914, Jackson Laboratories) to generate mice that expressed a red fluorescent protein in brain structures where *Nms* was expressed.

All procedures were approved by the Office of Animal Welfare at the University of Washington, Marquette University, or Oregon Health & Science University (OHSU).

Remaining Materials and Methods are described in *SI Appendix*.

Data, Materials, and Software Availability. Data used to generate figures data have been deposited in Github (https://github.com/delaiglesialab/Bussi-et-al.-2023) (40).

ACKNOWLEDGMENTS. This study was supported by R01 R01NS094211 and R03NS103111 to H.O.d.l.I. and NS103842 to C.N.A. A.F.N. received support from EY07031 Training Grant, and REAS received support from the Washington Research Foundation Innovation Graduate Fellowship in Neuroengineering. J.A.E. received support from R01GM143545. Portions of the paper were developed from the thesis of Dr. REAS.

Author affiliations: [a]Department of Biology, University of Washington, Seattle, WA 98195-1800; [b]Molecular and Cellular Biology in Seattle, University of Washington and Fred Hutch, Seattle, WA 98195-7275; [c]Graduate Program in Neuroscience, University of Washington, Seattle, WA 98195; [d]Oregon Institute for Occupational Health Sciences, Oregon Health & Science University, Portland, OR 97239; [e]Department of Behavioral Neuroscience, Oregon Health & Science University, Portland, OR 97239; and [f]Department of Biomedical Sciences, Marquette University, Milwaukee, WI 53233

Author contributions: I.L.B., A.F.N., R.E.A.S., C.N.A., J.A.E., and H.O.d.l.I. designed research; I.L.B., A.F.N., R.E.A.S., L.P.C., M.M., D.K., C.N.A., J.A.E., and H.O.d.l.I. performed research; A.F.N., C.N.A., J.A.E., and H.O.d.l.I. contributed new reagents/analytic tools; I.L.B., A.F.N., R.E.A.S., L.P.C., M.M., C.N.A., J.A.E., and H.O.d.l.I. analyzed data; and I.L.B. and H.O.d.l.I. wrote the paper.

1. M. H. Hastings, E. S. Maywood, M. Brancaccio, Generation of circadian rhythms in the suprachiasmatic nucleus. *Nat. Rev. Neurosci.* **19**, 453–469 (2018).
2. C. S. Colwell, Linking neural activity and molecular oscillations in the SCN. *Nat. Rev. Neurosci.* **12**, 553–569 (2011).
3. A. C. Liu *et al.*, Intercellular coupling confers robustness against mutations in the SCN circadian clock network. *Cell* **129**, 605–616 (2007).
4. E. D. Herzog, S. J. Aton, R. Numano, Y. Sakaki, H. Tei, Temporal precision in the mammalian circadian system: A reliable clock from less reliable neurons. *J. Biol. Rhythms* **19**, 35–46 (2004).
5. H. O. de la Iglesia, T. Cambras, W. J. Schwartz, A. Diez-Noguera, Forced desynchronization of dual circadian oscillators within the rat suprachiasmatic nucleus. *Curr. Biol.* **14**, 796–800 (2004).
6. J. H. Meijer, S. Michel, H. T. Vanderleest, J. H. Rohling, Daily and seasonal adaptation of the circadian clock requires plasticity of the SCN neuronal network. *Eur. J. Neurosci.* **32**, 2143–2151 (2010).
7. H. O. de la Iglesia, J. Meyer, A. Carpino Jr., W. J. Schwartz, Antiphase oscillation of the left and right suprachiasmatic nuclei. *Science* **290**, 799–801 (2000).
8. E. E. Abrahamson, R. Y. Moore, Suprachiasmatic nucleus in the mouse: Retinal innervation, intrinsic organization and efferent projections. *Brain Res.* **916**, 172–191 (2001).
9. R. Y. Moore, J. C. Speh, GABA is the principal neurotransmitter of the circadian system. *Neurosci. Lett.* **150**, 112–116 (1993).
10. B. Gao, R. Y. Moore, Glutamic acid decarboxylase message isoforms in human suprachiasmatic nucleus. *J. Biol. Rhythms* **11**, 172–179 (1996).
11. D. Ono, K. I. Honma, S. Honma, GABAergic mechanisms in the suprachiasmatic nucleus that influence circadian rhythm. *J. Neurochem.* **157**, 31–41 (2020). 10.1111/jnc.15012.
12. C. Liu, S. M. Reppert, GABA synchronizes clock cells within the suprachiasmatic circadian clock. *Neuron* **25**, 123–128 (2000).
13. S. Han *et al.*, NaV1.1 channels are critical for intercellular communication in the suprachiasmatic nucleus and for normal circadian rhythms. *Proc. Natl. Acad. Sci. U. S. A.* **109**, E368–E377 (2012).
14. J. A. Evans, T. L. Leise, O. Castanon-Cervantes, A. J. Davidson, Dynamic interactions mediated by nonredundant signaling mechanisms couple circadian clock neurons. *Neuron* **80**, 973–983 (2013).
15. K. E. Rohr *et al.*, Seasonal plasticity in GABAA signaling is necessary for restoring phase synchrony in the master circadian clock network. *Elife* **8**, e49578 (2019).
16. J. Myung *et al.*, GABA-mediated repulsive coupling between circadian clock neurons in the SCN encodes seasonal time. *Proc. Natl. Acad. Sci. U.S.A.* **112**, E3920–E3929 (2015).
17. D. DeWoskin *et al.*, Distinct roles for GABA across multiple timescales in mammalian circadian timekeeping. *Proc. Natl. Acad. Sci. U.S.A.* **112**, E3911–E3919 (2015).
18. G. M. Freeman Jr., R. M. Krock, S. J. Aton, P. Thaben, E. D. Herzog, GABA networks destabilize genetic oscillations in the circadian pacemaker. *Neuron* **78**, 799–806 (2013).
19. H. Albus, M. J. Vansteensel, S. Michel, G. D. Block, J. H. Meijer, A GABAergic mechanism is necessary for coupling dissociable ventral and dorsal regional oscillators within the circadian clock. *Curr. Biol.* **15**, 886–893 (2005).
20. S. J. Aton, J. E. Huettner, M. Straume, E. D. Herzog, GABA and Gi/o differentially control circadian rhythms and synchrony in clock neurons. *Proc. Natl. Acad. Sci. U.S.A.* **103**, 19188–19193 (2006).
21. D. Ono, K. I. Honma, Y. Yanagawa, A. Yamanaka, S. Honma, GABA in the suprachiasmatic nucleus refines circadian output rhythms in mice. *Commun. Biol.* **2**, 232 (2019).
22. W. D. Todd *et al.*, Suprachiasmatic VIP neurons are required for normal circadian rhythmicity and comprised of molecularly distinct subpopulations. *Nat Commun* **11**, 4410 (2020).
23. T. Maejima *et al.*, GABA from vasopressin neurons regulates the time at which suprachiasmatic nucleus molecular clocks enable circadian behavior. *Proc. Natl. Acad. Sci. U.S.A.* **118**, e2010168118 (2021).
24. I. T. Lee *et al.*, Neuromedin s-producing neurons act as essential pacemakers in the suprachiasmatic nucleus to couple clock neurons and dictate circadian rhythms. *Neuron* **85**, 1086–1102 (2015).
25. T. A. LeGates *et al.*, Aberrant light directly impairs mood and learning through melanopsin-expressing neurons. *Nature* **491**, 594–598 (2012).
26. J. S. Marvin *et al.*, A genetically encoded fluorescent sensor for in vivo imaging of GABA. *Nat Methods* **16**, 763–770 (2019).
27. M. Mieda, The central circadian clock of the suprachiasmatic nucleus as an ensemble of multiple oscillatory neurons. *Neurosci. Res.* **156**, 24–31 (2020).
28. S. Wen *et al.*, Spatiotemporal single-cell analysis of gene expression in the mouse suprachiasmatic nucleus. *Nat. Neurosci.* **23**, 456–467 (2020).
29. S. J. Aton, C. S. Colwell, A. J. Harmar, J. Waschek, E. D. Herzog, Vasoactive intestinal polypeptide mediates circadian rhythmicity and synchrony in mammalian clock neurons. *Nat. Neurosci.* **8**, 476–483 (2005).

30. E. S. Maywood *et al.*, Synchronization and maintenance of timekeeping in suprachiasmatic circadian clock cells by neuropeptidergic signaling. *Curr. Biol.* **16**, 599–605 (2006).
31. M. Moldavan, O. Cravetchi, C. N. Allen, Diurnal properties of tonic and synaptic GABAA receptor-mediated currents in suprachiasmatic nucleus neurons. *J. Neurophysiol.* **126**, 637–652 (2021).
32. R. Silver, J. LeSauter, P. A. Tresco, M. N. Lehman, A diffusible coupling signal from the transplanted suprachiasmatic nucleus controlling circadian locomotor rhythms. *Nature* **382**, 810–813 (1996).
33. A. C. Rupp *et al.*, Distinct ipRGC subpopulations mediate light's acute and circadian effects on body temperature and sleep. *Elife* **8**, e44358 (2019).
34. N. J. Kingsbury, S. R. Taylor, M. A. Henson, Inhibitory and excitatory networks balance cell coupling in the suprachiasmatic nucleus: A modeling approach. *J. Theor. Biol.* **397**, 135–144 (2016).
35. A. J. Harmar *et al.*, The VPAC(2) receptor is essential for circadian function in the mouse suprachiasmatic nuclei. *Cell* **109**, 497–508 (2002).
36. T. W. Lin *et al.*, Regulation of synapse development by Vgat deletion from ErbB4-positive interneurons. *J. Neurosci.* **38**, 2533–2550 (2018).
37. V. Carmona-Alcocer *et al.*, Ontogeny of circadian rhythms and synchrony in the suprachiasmatic nucleus. *J. Neurosci.* **38**, 1326–1334 (2018).
38. J. A. Evans, H. Pan, A. C. Liu, D. K. Welsh, Cry1$^{-/-}$ circadian rhythmicity depends on SCN intercellular coupling. *J. Biol. Rhythms* **27**, 443–452 (2012).
39. T. Yoshikawa, S. Yamazaki, M. Menaker, Effects of preparation time on phase of cultured tissues reveal complexity of circadian organization. *J. Biol. Rhythms* **20**, 500–512 (2005).
40. I. L. Bussi, H. O. de la Iglesia, Bussi-et-al.-2023. Github. https://github.com/delaiglesialab/Bussi-et-al.-2023. Deposited 29 October 2023.